

# On-wafer spectrofluorometric evaluation of the response of photoacid generator compounds in chemically amplified photoresists

G. D. Feke, D. Hessman,<sup>a)</sup> and R. D. Grober<sup>b)</sup>

Department of Applied Physics, Yale University, New Haven, Connecticut 06520-8284

B. Lu and J. W. Taylor

Center for NanoTechnology, University of Wisconsin-Madison, Stoughton, Wisconsin 53589-3097

(Received 26 August 1999; accepted 22 October 1999)

The enhanced photospeed of chemically amplified photoresists is crucial for high throughput lithography required by the semiconductor industry. The photospeed depends directly on the efficiency of the generation of photoacid during exposure, which is a function of the properties of the photoacid generator compound used in the resist. We report a novel technique for photoacid generator evaluation which is convenient, fast, and robust. This technique involves “whole wafer” imaging of resist doped with pH-sensitive fluorophores and patterned with an array of fields of varying doses. A spatially encoded map of the response of the compound under study is thus obtained in a single camera image. We measure the amount of photoacid produced as a function of dose for three photoacid generator compounds with reference to the commercial resist Shipley SAL 605. The results demonstrate a one-to-one correspondence with lithographic performance as determined by the normalized remaining thickness technique. © 2000 American Vacuum Society. [S0734-211X(00)05201-X]

## I. INTRODUCTION

A principal advantage of chemically amplified photoresists<sup>1</sup> for semiconductor lithography is their increased photospeed. In this class of resists a catalyst, typically a strong acid, is generated during exposure by photolysis of a photoacid generator (PAG) compound.<sup>2</sup> The efficiency of photoacid generation depends on the properties, such as chemical structure and molecular weight, of the particular PAG used in the resist, and is quantified by the amount of photoacid created per exposure dose. The photoacid catalytically generates linking or deprotection reactions during a postexposure bake (PEB) of the resist. The amplification occurs during PEB with the multiple recycling of the photoacid to promote many chemical reactions. The photospeed depends on the product of the yields of these two steps.

The concentration of photoacid in chemically amplified resists is typically measured by absorption or fluorescence spectroscopy of pH indicators. Spectrophotometric and spectrofluorometric titration techniques have used merocyanine dye,<sup>3,4</sup> tetrabromophenol blue,<sup>5-10</sup> rhodamine B base,<sup>11,12</sup> benzothiazole dyes,<sup>11,12</sup> fluorescein,<sup>11-13</sup> aromatic monoazines,<sup>14</sup> and the Rhodol derivative CI-NERF<sup>15,16</sup> as indicators. Generally, spectroscopic measurements are obtained *in vitro* by means of dissolution of exposed resist films. Several studies have demonstrated *in situ* measurements of photoacid concentration in exposed films.<sup>11,12,14-16</sup> We herein report a novel extension of the optical titration technique which enables *in situ* mapping of resist response with a “single shot” measurement. This technique involves fluorescence imaging of an entire wafer, coated with resist

which contains a dilute concentration of pH-sensitive fluorescent molecules, and patterned with fields of various exposure doses. The imaging aspect of the technique provides spectrofluorometric titration “in parallel,” with the advantages of convenience, speed, and robustness.

## II. THEORY

Although optical titration techniques are well understood (see Ref. 17 for example), a review of the measurement theory is appropriate here. For a single-step titration, the fluorescence intensity  $F$  measured from an ensemble of molecules is given by

$$F = F_{B^-}c_{B^-} + F_{BH}c_{BH}. \quad (1)$$

Here  $F_{B^-}$  ( $F_{BH}$ ) is the fluorescence intensity that would be obtained if all the molecules were in their native (protonated) state. These quantities would typically be obtained from the alkaline (acidic) ends of a spectrofluorometric titration curve.  $c_{B^-}$  ( $c_{BH}$ ) is the fractional concentration of the native (protonated) fluorophores, respectively, ( $c_{B^-} + c_{BH} = 1$ ). These concentrations vary with pH according to

$$K_a = \frac{hc_{B^-}}{c_{BH}}, \quad (2)$$

where  $K_a$  (where  $pK_a = -\log K_a$ ) is the mixed dissociation constant, and  $h$  is the hydrogen ion activity, defined as the ratio of the hydrogen ion concentration,  $[H^+]$ , to a 1 M concentration. Strictly speaking, the quantity pH is defined as the negative of the logarithm of the hydronium ion ( $H_3O^+$ ) activity in an aqueous solution. We measure  $[H^+]$  in units of moles of  $H^+$  per cubic centimeter and convert to moles per liter (using  $1000 \text{ cm}^3/\text{L}$  for  $H_2O$ ) to define an effective  $pH = -\log h$ .

<sup>a)</sup>Present address: Dept. of Solid State Physics, Lund University, Box 118, S-221 00 Lund, Sweden.

<sup>b)</sup>Electronic mail: robert.grober@yale.edu

For a molecule whose emission decreases in an acidic environment ( $0 < F_{\text{BH}} < F_{\text{B}^-}$ ), we define the fractional fluorescence  $f = F/F_{\text{B}^-}$  and the protonated/native fluorescence ratio  $f_R = F_{\text{BH}}/F_{\text{B}^-}$ . Therefore,  $0 < f \leq 1$  and  $0 < f_R < 1$ . The fractional fluorescence can therefore be expressed as

$$f = \frac{f_R h + K_a}{h + K_a} \quad (3)$$

Equation (3) yields the titration curve. Measurement of  $f_R$  and  $K_a$  from titration data allows the direct correspondence between  $f$  and  $h$ .

### III. EXPERIMENT

To measure  $f$  as a function of exposure dose, and hence, evaluate the efficiency of PAG compounds, we developed the following technique. A dilute concentration of fluorophore is added to the casting solutions of the resists. The fluorophore chosen for this study was Cl-NERF (Molecular Probes, Eugene, OR).<sup>18</sup> Four criteria influenced our selection: (1) the excitation and emission spectra of the fluorophore (with peaks centered at 515 and 545 nm, respectively) lie in regions where the resist is photochemically passive, (2) the  $pK_a$  of the fluorophore in the photoresist matrix matches to the  $pH$  range of the resists under study, (3) the fluorophore does not photobleach very quickly, and (4) the addition of the fluorophore does not significantly alter the chemistry of the resist.<sup>15,16</sup> The emission of this molecule quenches upon protonation:  $F_{\text{BH}} < F_{\text{B}^-}$ . Although the emission of Cl-NERF extends to 650 nm, we have determined that the spectrum is sensitive to  $pH$  in the wavelength range 530–560 nm. The details of this measurement will be presented in a future publication.

We chose three PAGs for comparison in this report: 4,4'-isopropylidenebis(2,6-di-bromophenol) (TBBPA), 4,4'-isopropylidenebis(2,6-di-chlorophenol) (TCBPA), and pentabromophenol (PBP) (Aldrich, Milwaukee, WI). The structures of these compounds are described elsewhere.<sup>19</sup> Each compound produces a hydrogen halide during exposure. For reference, we also studied the commercial resist SAL 605 (Shipley Co., Marlborough, MA), which produces HBr.<sup>20</sup> The three experimental negative-tone x-ray/e-beam resists were made using novolac resin (Schenectady Int., Schenectady, NY) as the base polymer, hexamethoxymethylmelamine product Cymel 300 (American Cyanamid, Wayne, NJ) as the linking reagent, and each of the PAGs listed earlier. These formulations are similar to SAL 605. We added 0.07 wt % (versus solids content) of Cl-NERF to the casting solutions of the four resists. The resists were spun onto 4 in. silicon wafers as 0.5  $\mu\text{m}$  films. We conducted postapply bakes at 118 °C for 72 s. For fair comparison, we added all PAGs in the same moles to solids ratio to the casting solutions. The exposures were done at the Center for NanoTechnology at the University of Wisconsin-Madison on the ES-5 beam line connected to a Karl Suss XRS 200/2M x-ray stepper. We patterned each wafer with an array of nine 9 × 9 mm squares with doses varying from 40 to 900 mJ/cm<sup>2</sup>. The exposure doses reported are to a 2  $\mu\text{m}$  silicon nitride

membrane. The membrane absorbs approximately 50% of the radiation at the exposure wavelength, so the dose to the resists is approximately half of the dose to the membrane.

PEB has been observed to effect an increase of the amount of quenching for a given exposure dose.<sup>16</sup> One possible explanation is that following photogeneration, some fraction of the acid is trapped on the nitrogen sites of the linking molecule, which are the most basic sites in the resist+fluorophore system.<sup>21</sup> This fraction is then released during PEB to catalyze linking reactions. For Cl-NERF in SAL 605, we have determined that the amount of quenching increases after approximately 10 s of PEB at 108 °C. We conducted 60 s PEBs on the wafers in order to both obtain this increased fluorescence contrast and to perform a comparison of the lithographic performance subsequent to the fluorescence experiment. The wafers were placed in a wafer box packed with approximately 10 g of molecular sieves (5 g each of 5 Å, Union Carbide, Plainfield, NJ, and 4 Å, Matheson Coleman, Norwood, OH), outgassed with dry nitrogen, and sealed before overnight shipment to Yale University.

The wafers are analyzed with a "whole wafer" fluorescence imaging apparatus constructed at Yale University. We illuminate the entire area of each of the wafers with the 514.5 nm line of an Ar ion laser (Coherent, Palo Alto, CA) in order to excite the fluorophores in all of the dose fields. The illumination is performed by coupling the laser beam into a single mode optical fiber, and collimating the fiber output [transverse electromagnetic (TEM)<sub>00</sub> mode] with a 4 in. diameter lens. The angle of incidence onto the wafer is 30° with respect to the surface normal. We image the wafer onto a thermoelectrically cooled charge coupled device (CCD) camera (RS Princeton Instruments, Trenton, NJ) with 1152 × 298 22.5  $\mu\text{m}$  square pixels (25.9 × 6.7 mm image size) and 16 bit resolution. The demagnification is 9 × (i.e., magnification of 0.11 ×). The optical axis of the collection beam-path is normal to the wafer. The wafer surface specularly reflects the excitation light away from the collection optics. To provide suppression of the small amount of scattered excitation light from surface contaminants, we insert a 514.5 nm holographic notch filter (Kaiser Optical Systems, Inc., Ann Arbor, MI) into the collection beam-path. We also insert a 530–560 nm bandpass filter (Omega Optical, Inc., Brattleboro, VT) into the collection beam-path to reject the  $pH$ -insensitive emission for above 560 nm, thereby optimizing the contrast of the image. We imaged each of the four wafers using an integration time of 300 s in order to use the full dynamic range of the camera (with the given excitation intensity). Each dose field was imaged onto 43 × 43 pixels. Occasionally a small speck of dust would appear in the field of view; in such a case we removed the affected pixels from the fitting data set.

### IV. RESULTS AND DISCUSSION

An example of the fluorescence image we obtain is shown in Fig. 1. Each of the fields of different doses exhibits a different degree of fluorescence quenching with respect to the unexposed region around the fields. To obtain the data

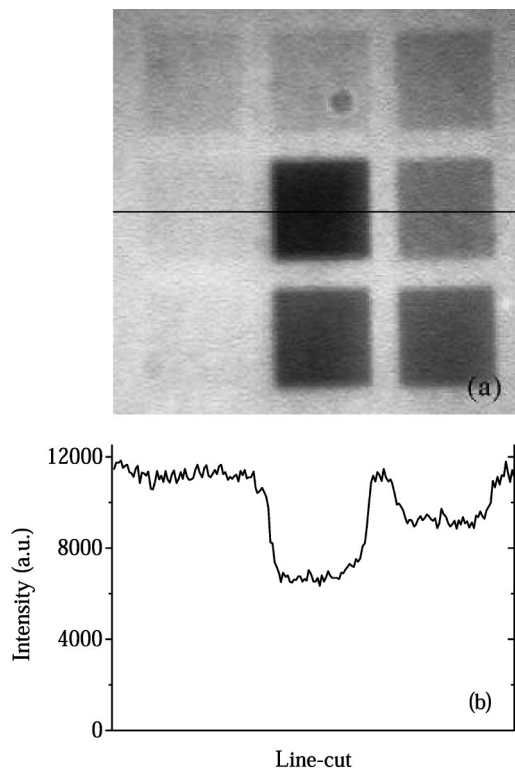


FIG. 1. Image of a wafer obtained by the fluorescence telescope is shown in (a). The PAG is TBBPA. Clockwise from lower left, the exposure doses of the fields (measured to a silicon nitride membrane) are 40, 60, 80, 120, 180, 300, 500, 700, and 900  $\text{mJ}/\text{cm}^2$  in the center. Each of the exposed fields is  $9 \times 9$  mm. The line cut in (b) is taken from the horizontal black line drawn over the image.

for PAG efficiency evaluation, we normalize the measured fluorescence intensity from the pixels composing each of the dose fields in the image by the intensity measured from the unexposed area. The analysis was conducted on the four wafers, and the normalized intensity (NI) results are shown in Fig. 2. The results show that the amount of quenching, and hence the efficiency, of the PAGs is in series of TBBPA > TCBPA > PBP, and SAL 605 is the most efficient.

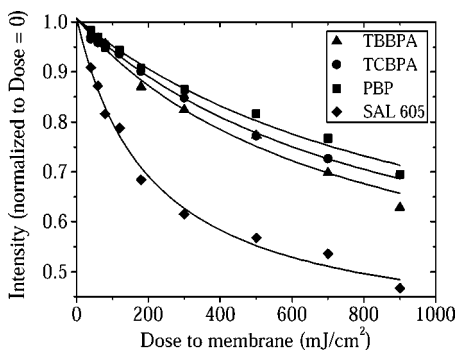


FIG. 2. Fluorescence vs dose for the PAGs, TBBPA, TCBPA, PBP, and SAL 605. The data for each PAG is obtained simultaneously using the whole wafer imaging technique. The intensity measured for each exposed field is normalized by the intensity of the unexposed background. The lines are obtained from the results of fits to Eq. (4).

TABLE I. PAG efficiency comparison.

PAG	Efficiency $\phi$ (relative to SAL 605)	$\alpha$ ( $10^{-5} \text{ cm}^2/\text{mJ}$ )
SAL 605	1	4.03
TBBPA	$0.27 \pm 0.02$	$1.09 \pm 0.08$
TCBPA	$0.23 \pm 0.01$	$0.93 \pm 0.04$
PBP	$0.19 \pm 0.01$	$0.77 \pm 0.04$

Using spectrophotometric titration of tetrabromophenol blue, Dentinger found that the photogenerated acid activity is a linear function of exposure dose for SAL 605:  $h = \alpha \cdot \text{Dose}$ , where  $\alpha = 4.03 \times 10^{-5} \text{ cm}^2/\text{mJ}$ .<sup>10</sup> Also, the pH of unexposed SAL 605 has been measured to be approximately 4.0.<sup>22</sup> Using the formalism described earlier, the NI data of Fig. 2 are given by  $F(h)/F(h_{\text{unexposed}})$ , where  $h_{\text{unexposed}} = 10^{-4.0}$  is assumed to be constant for each resist. This expression is equivalent to  $f(h)/f(h_{\text{unexposed}})$ . We therefore convert the Dose coordinate to an  $h$  coordinate and simultaneously fit each of the data sets of Fig. 2 to

$$\text{NI} = \frac{(f_R \phi h + K_a) / (\phi h + K_a)}{(f_R h_{\text{unexposed}} + K_a) / (h_{\text{unexposed}} + K_a)}. \quad (4)$$

Here  $f_R$  and  $K_a$  are free parameters shared between each of the four fits (we assume that these quantities are constants of the fluorophore and independent of the resist). The scale factor  $\phi$  is set equal to one for the fit of the data of the reference resist SAL 605, and is a free parameter for each of the fits to the data of the experimental resists ( $\phi$  is not shared). The parameter  $\phi$  is therefore the relative efficiency of each PAG with respect to SAL 605.

The fit curves are shown as the solid lines in Fig. 2. For the shared parameters, we obtain  $f_R = 0.36$  and  $K_a = 0.0084$  ( $pK_a = 2.08$ ). The relative errors in these measurements are  $\delta f_R / f_R = 0.05$  and  $\delta K_a / K_a = 0.08$ . Vendor data for titration of Cl-NERF in aqueous buffers yields  $f_R = 0.097$  and  $pK_a = 3.74$ .<sup>23</sup> Since  $pK_a$  is essentially a measurement of the reactivity of the hydrogen ions with the fluorophores, the lower  $pK_a$  obtained from our measurement compared with the value measured from aqueous buffers may be explained by the fact that the fluorophores are immobilized in the resist matrix. The discrepancy in the  $f_R$  measurement may also be due to the fluorophore immobilization.

The results for  $\phi$  for each of the data sets are given in Table I. Using the result of Ref. 10, the constant of proportionality  $\alpha$  between photogenerated acid activity and exposure dose can be obtained for the experimental PAGs. These calculations are also given in Table I. The results can be explained as follows. The different halogen groups of PAGs have a different leaving ability or a different stability of halogen radicals formed during the exposure. Normally, the bond dissociation energy of the C-Br bond is less than the C-Cl bond. For example, the dissociation energies of  $\text{CH}_3\text{-Br}$  and  $\text{CH}_3\text{-Cl}$  are 70 and 84 kcal/mol, respectively.<sup>24</sup> The lower the dissociation energy is, the easier the halogen leaves, and the easier the halogen radical can form, therefore, the more hydrogen halide forms. Given a certain energy, the

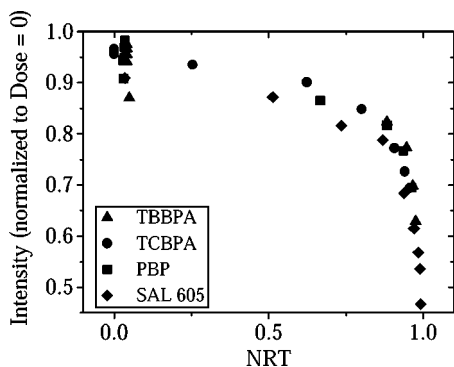


FIG. 3. Plot of the spectrofluorometric data vs the NRT data for each resist. All the data lie on the same curve, which implies that there is a one-to-one correspondence between the two techniques.

compound with lower halogen-carbon bond dissociation energy would generate more hydrogen halide. The volatility of hydrogen halides may also contribute to the quenching efficiency. Therefore, TBBPA has a higher efficiency than TCBPA. On the other hand, while PBP contains five Br groups, it is possible that only the para- and ortho- Br vs -OH groups are active. TBBPA has four active Br groups. Therefore, one expects TBBPA to be a more efficient PAG. A more detailed discussion is published elsewhere.<sup>19</sup>

These PAGs and SAL 605 were also compared based on their lithographic performance. The normalized remaining thickness (NRT) technique was applied to the same wafers which underwent spectrofluorometric evaluation. The NRT measurement is the ratio of the resist thickness after development to the thickness before development (essentially a measurement of the dissolution rate), and is generally used to determine resist sensitivity and contrast. The NRT results yielded the same ordering of the efficiency of the PAGs, and are published elsewhere.<sup>19</sup> In Fig. 3 we plot the spectrofluorometric data against the NRT data for each resist and find that all the data lie on the same curve. This indicates a one-to-one correspondence between the two techniques. This is not surprising given that the dissolution rate is a function of  $[H^+]$ ,<sup>25</sup> as is the normalized intensity. The fact that all the data fall on the same curve implies that all the other parameters which effect the NI and NRT measurements (such as fluorophore response, reaction rates, etc.) are constant across the resists studied.

## V. SUMMARY

We have developed a novel, on-wafer technique for evaluation of the efficiency of PAG compounds using spectrofluorometric imaging. We have demonstrated the evalua-

tion and comparison of three PAGs and SAL 605. The advantages of this technique are its speed, convenience, and robustness. These advantages are important for the application of this technique to rapid screening of new compounds to determine usefulness as PAGs and the comparison of not only different PAGs, but differing amounts of each PAG.

## ACKNOWLEDGMENTS

The authors thank James Cameron for helpful discussions. We also thank Qiang Wu for generously donating the use of the CCD camera. This work is supported by the Semiconductor Research Corporation, SRC Grant Nos. 98-LJ-438 and 98-LP-452, and by DARPA/ONR Grant No. N-00014-97-1-0460. The Synchrotron Radiation Center is supported by the National Science Foundation under Grant No. DMR-95-31009.

- <sup>1</sup>D. Seeger, *Solid State Technol.* **40**, 115 (1997).
- <sup>2</sup>S. P. Pappas, *J. Imaging Technol.* **11**, 146 (1985).
- <sup>3</sup>P. J. Paniez, D. C. Demattei, and M. J. M. Abadie, *Microelectronics* **17**, 279 (1992).
- <sup>4</sup>D. R. McKean, R. D. Allen, P. H. Kasai, U. P. Schaedeli, and S. A. MacDonald, *Proc. SPIE* **1672**, 94 (1992).
- <sup>5</sup>T. H. Fedynyshyn, J. W. Thackeray, J. H. Georger, and M. D. Denison, *J. Vac. Sci. Technol. B* **12**, 3888 (1994).
- <sup>6</sup>K. Asakawa, T. Ushirogouchi, and M. Nakase, *Proc. SPIE* **2438**, 563 (1995).
- <sup>7</sup>N. Kihara, S. Saito, T. Ushirogouchi, and M. Nakase, *J. Photopolym. Sci. Technol.* **8**, 561 (1995).
- <sup>8</sup>J. F. Cameron, A. J. Orelan, M. M. Rajaratnam, and R. F. Sinta, *Proc. SPIE* **2724**, 261 (1996).
- <sup>9</sup>T. Itani, H. Yoshino, S. Hashimoto, M. Yamana, N. Samoto, and K. Kasama, *J. Vac. Sci. Technol. B* **14**, 4226 (1996).
- <sup>10</sup>P. M. Dentinger, C. M. Nelson, S. J. Rhyner, J. W. Taylor, T. H. Fedynyshyn, and M. F. Cronin, *J. Vac. Sci. Technol. B* **14**, 4239 (1996).
- <sup>11</sup>G. Pohlert, J. C. Scaiano, and R. Sinta, *Chem. Mater.* **9**, 3222 (1997).
- <sup>12</sup>J. F. Cameron *et al.*, *Proc. SPIE* **3333**, 680 (1998).
- <sup>13</sup>A. R. Eckert and W. M. Moreau, *Proc. SPIE* **3049**, 879 (1997).
- <sup>14</sup>G. Pohlert, S. Virdee, J. C. Scaiano, and R. Sinta, *Chem. Mater.* **8**, 2654 (1996).
- <sup>15</sup>S. J. Bukofsky, G. D. Feke, Q. Wu, R. D. Grober, P. M. Dentinger, and J. W. Taylor, *Appl. Phys. Lett.* **73**, 408 (1998).
- <sup>16</sup>P. M. Dentinger, B. Lu, J. W. Taylor, S. J. Bukofsky, G. D. Feke, D. Hessman, and R. D. Grober, *J. Vac. Sci. Technol. B* **16**, 3767 (1998).
- <sup>17</sup>J. Polster and H. Lachmann, *Spectrometric Titrations* (VCH, New York, 1989).
- <sup>18</sup>J. E. Whitaker, R. P. Haugland, D. Ryan, P. C. Hewitt, R. P. Haugland, and F. G. Prendergast, *Anal. Biochem.* **207**, 267 (1992).
- <sup>19</sup>B. Lu, P. M. Dentinger, J. W. Taylor, G. D. Feke, D. Hessman, Q. Wu, and R. D. Grober, *Proc. SPIE* **3676**, 466 (1999).
- <sup>20</sup>T. H. Fedynyshyn, M. F. Cronin, L. C. Poli, and C. Kondek, *J. Vac. Sci. Technol. B* **8**, 1454 (1990).
- <sup>21</sup>J. F. Cameron (private communication).
- <sup>22</sup>P. M. Dentinger, Ph.D. dissertation, UW-Madison, 1998.
- <sup>23</sup>C. Walker (private communication).
- <sup>24</sup>R. T. Morris and R. N. Boyd, *Organic Chemistry*, 6th ed. (Prentice Hall, Englewood Cliffs, NJ, 1992).
- <sup>25</sup>T. H. Fedynyshyn, C. R. Szmanda, R. F. Blacksmith, W. E. Houck, and J. C. Root, *J. Vac. Sci. Technol. B* **11**, 2798 (1993).